



## Acceleration of protons to above 6 MeV using H<sub>2</sub>O "snow" nanowire targets

I. Pomerantz, E. Schleifer, E. Nahum, S. Eisenmann, M. Botton, D. Gordon, P. Sprangel, and A. Zigler

Citation: [AIP Conference Proceedings](#) **1462**, 159 (2012); doi: 10.1063/1.4736782

View online: <http://dx.doi.org/10.1063/1.4736782>

View Table of Contents: <http://scitation.aip.org/content/aip/proceeding/aipcp/1462?ver=pdfcov>

Published by the [AIP Publishing](#)

---

### Articles you may be interested in

[Response functions of Fuji imaging plates to monoenergetic protons in the energy range 0.6–3.2 MeV](#)  
Rev. Sci. Instrum. **84**, 013508 (2013); 10.1063/1.4775719

[Hundreds MeV monoenergetic proton bunch from interaction of 1020–21 W/cm<sup>2</sup> circularly polarized laser pulse with tailored complex target](#)  
Appl. Phys. Lett. **100**, 134103 (2012); 10.1063/1.3696885

[Estimated interaction and proton removal cross sections for 60 – 710 A MeV <sup>15</sup>O and <sup>17</sup>Ne nuclei on <sup>9</sup>Be and <sup>12</sup>C targets](#)  
AIP Conf. Proc. **831**, 526 (2006); 10.1063/1.2201004

[Production of a MeV proton with 30 mJ laser energy by optimizing the focusing spot using a deformable mirror](#)  
Rev. Sci. Instrum. **76**, 073305 (2005); 10.1063/1.1942527

[An intense, compact fourth-generation positron source based on using a 2 MeV proton accelerator](#)  
AIP Conf. Proc. **576**, 741 (2001); 10.1063/1.1395413

---

# Acceleration of Protons to Above 6 MeV using H<sub>2</sub>O "Snow" Nanowire Targets

I. Pomerantz<sup>a</sup>, E. Schleifer<sup>b</sup>, E. Nahum<sup>b</sup>, S. Eisenmann<sup>b</sup>, M. Botton<sup>b</sup>,  
D. Gordon<sup>c</sup>, P. Sprangel<sup>c</sup> and A. Zigler<sup>b</sup>

(a) Department of Physics, Texas Center for High Intensity Laser Science, The University of Texas at Austin,  
Austin, Texas 78712, USA

(b) Racah Institute of Physics, Hebrew University, Jerusalem 91904, Israel

(c) Plasma Physics Division, Naval Research Laboratory, Washington, D.C. 20375, USA

**Abstract.** A scheme is presented for using H<sub>2</sub>O "snow" nanowire targets for the generation of fast protons. This novel method may relax the requirements for very high laser intensities, thus reducing the size and cost of laser based ion acceleration system.

Compact sources of high energy protons (50-500MeV) are expected to play key role in a wide range of scientific applications [1-3]. In general, laser intensities exceeding  $10^{18}$  W/cm<sup>2</sup> are required to produce MeV level protons. Particularly promising is the Target Normal Sheath Acceleration (TNSA) scheme [4-5] for ion acceleration, holding a record level of generating 67 MeV protons using a Petawatt laser [6]. Enhancing the generated protons energy spectra using compact laser sources is a very attractive goal nowadays. Recently, the use of nanometer scale targets to generate high energy ions has been investigated [7,8]. Here we report on the first generation of 5.5-7.5 MeV protons by modest laser intensities of  $4.5 \times 10^{17}$  W/cm<sup>2</sup> interacting with nanometer-sized frozen water droplets (snow nanowires) deposited on a Sapphire substrate and the generation of 12 MeV protons in laser intensities of  $1.5 \times 10^{18}$  W/cm<sup>2</sup> [9-10,12]. In this setup, the plasma near the tip of the nanowire is subjected to a local enhancement of the laser intensity with high spatial gradients, and confined charge separation is obtained. Electrostatic fields of extremely high intensities are produced, and protons are accelerated to MeV-level energies.

In this setup, the target is positioned at the focal point of an 0.5 TW laser, with 40 fsec pulse duration, at the Hebrew University High Intensity Laser facility. Fig. 1 presents the schematics of the experimental setup. The laser operates at a central wavelength of 798 nm, and is focused by an off-axis parabolic mirror (F/3.3) to a spot area of 80  $\mu\text{m}^2$  (FWHM) on the target. The laser irradiates the snow interface at 60° normal to the target surface. A pre-pulse of time duration similar to the main pulse, originates in the regenerative pre-amplifier, and precedes the main pulse by 10 nsec. The main pulse to pre-pulse contrast ratio is  $10^3$ . A microscopic imaging system is used to make sure that the laser irradiates a fresh patch of snow at every shot.

Two sets of diagnostics are used to measure the accelerated protons energy spectrum. The first consists of CR39 SSNTD plates, covered by various layers of Mylar and Aluminum foils serving as energy filters. The detector is positioned at a distance of 35 mm from the target's plane along the normal, collecting protons from solid angle of 1.2 sr. A reference CR39 detector is placed at a position hidden from the target to measure the background signal. Each detector with energy filter setup is exposed to a series of 30-50 laser shots before being pulled out of the vacuum chamber and processed. The protons energy spectrum was also measured by a Time Of Flight (TOF) spectrometer, which consists of a scintillating plastic (BC-400)

detector coupled to a Photomultiplier Tube (PMT). The detector is placed at the end of a drift pipe, at a distance of 1.06 m from the target.

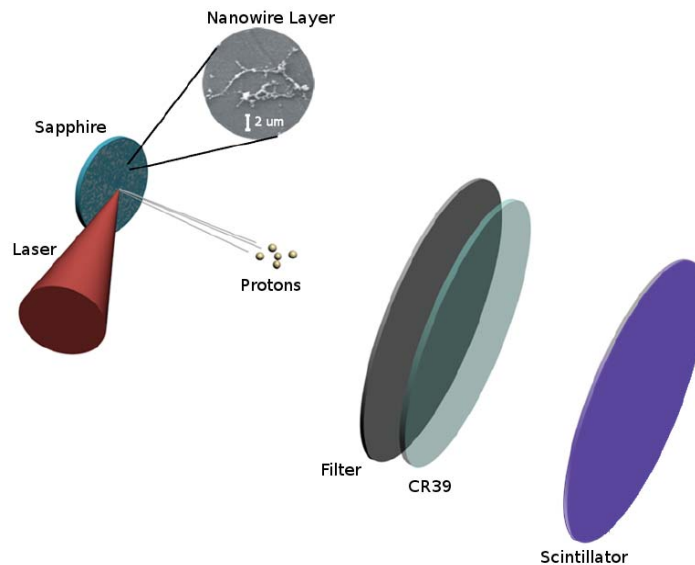


**FIGURE 1.** Schematics of the experimental setup

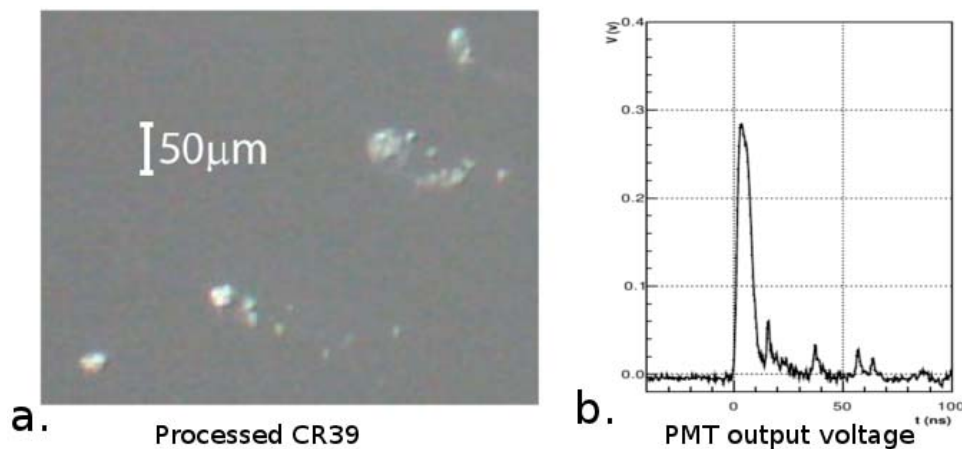


**FIGURE 2.** (a) Proton track bunches on a processed CR39 plate. (b) Typical PMT output voltage for a shot. The peak at  $t=0$  ns is the signal of the prompt x-ray and high energy electrons emerging from the target.

A typical scan of the processed CR39 detector is shown in Fig. 2a. The proton tracks (bright, circular spots) are accumulated in bunches, with no preferred orientation on the detector plane. Proton bunches are accelerated into relatively small solid angles of about  $1.6 \mu\text{sr}$ . We therefore deduce that a bunch represents several protons accelerated in one shot at the same direction. Considering the stopping power of the aluminum foil (of thickness  $208 \mu\text{m}$ ) that is placed in front of the CR39 detector, we conclude that the energy of the fastest protons is 5.5-7.5 MeV [14]. A typical PMT output voltage is shown in Fig. 2b. The peak at  $t=0$  ns is the signal of prompt x-ray and MeV-level electrons.

The number of proton tracks behind the filters is  $4708 \pm 707$  protons/shot/sr compared to a background level of  $2942 \pm 1079$  on the unexposed CR39. Note that the detector is placed at

an angle to the laser beam thus the protons are not accelerated along the laser direction as in the planar TNSA experiments.

The TOF experiments were done using a spot size of  $20 \mu\text{m}^2$  and the intensity of  $1.5 \times 10^{18} \text{ W/cm}^2$ . Peaks in the PMT output spectra which are 1 sigma over the background were chosen for the analysis. Fig.3 shows a PMT output voltage spectra integrated over  $\sim 100$  shots, for runs without (a) and with (b) the CR39 plate obscuring the scintillator from the target. The structure centered at  $t=24 \text{ ns}$  which corresponds to 12 MeV protons in (a) is shifted to  $t=28 \text{ ns}$  which corresponds to 8 MeV protons. This decrease of the proton energy matches the expected attenuation in the CR39.

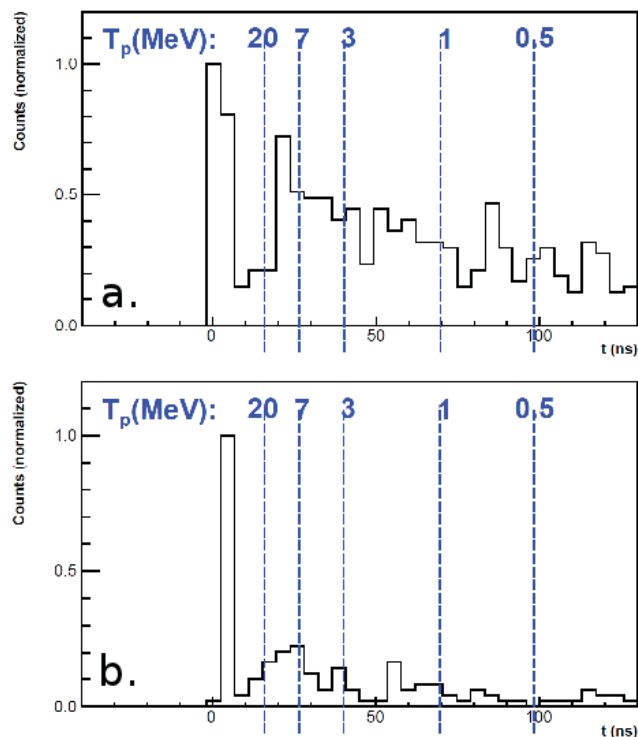


**FIGURE 3.** PMT output voltage integrated over  $\sim 100$  shots without (a) and with (b) a CR39 plate obscuring the target from the scintillator.

The scaling of the protons energy as a function of the intensity of the main pulse is shown in Fig. 4. The data obtained in the current experiments (HU) follows the conventional relation  $E_{\text{max}} \propto (I\lambda^2)^{0.5}$ , but is achieved with lower laser energy and intensity levels.

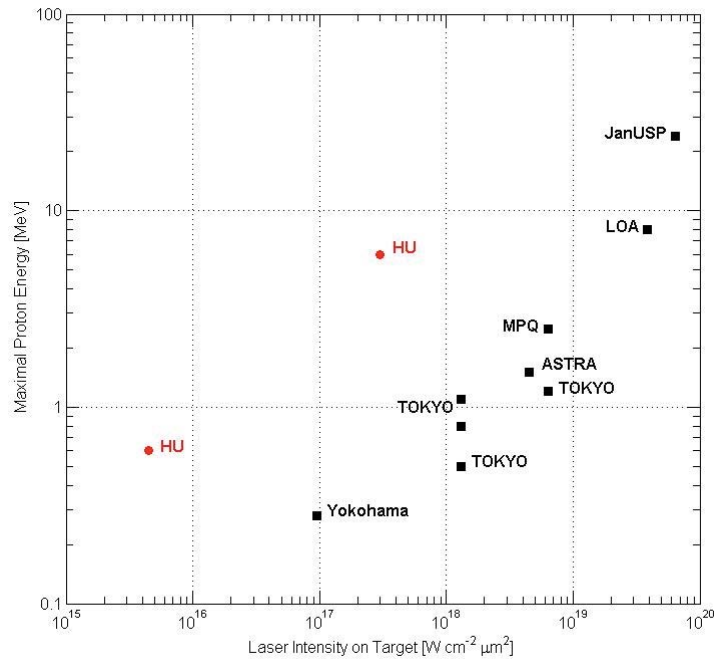


**FIGURE 4.** Maximal proton energy achieved in acceleration experiments using a short (<100 fsec) pulse Ti: Sapphire laser systems (Data taken from Refs [3,11])

A possible explanation of the experimental results starts with the assumption that the arrangement of the nanowires on the target is amorphous due to the deposition method. For simplicity, we assume that the laser (pre-pulse and main pulse) interacts with only one nanowire. The highly efficient absorption of the laser energy by the snow target [9] points to the fact that the pre-pulse completely vaporizes the nanowire (note that the plasma skin depth is larger than the width of the nanowire). The temperature of the formed plasma is estimated to be about 2-5eV. During the 10nsec interval between the pre-pulse and the main pulse, the plasma freely expands away from the nanowire. The main pulse therefore interacts with a non-uniform cylindrical symmetric plasma density (see Fig. 5), unlike the conventional TNSA foil configuration where the laser interacts with constant or planar plasma distribution.

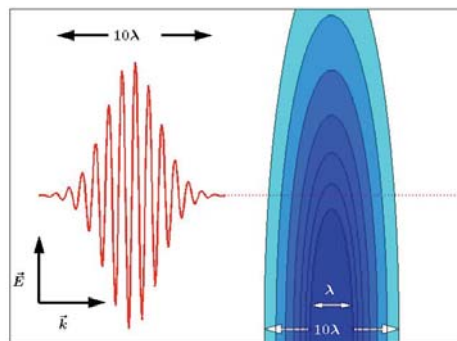


**FIGURE 5.** Model - The plasma density (Darker blue represents higher density) in the vicinity of the H2O nanowire at the time the main pulse (red on the left) impinges the target

For brevity of presentation, the main laser pulse is assumed to propagate in a direction perpendicular to the needle symmetry axis. Even with these simplifications the interaction is essentially three dimensional as the laser breaks the cylindrical symmetry of the nanowire.

The main-pulse length is larger than the width of the nanowire. Accordingly the averaged ponderomotive potential of the laser in the vicinity of the tip can be calculated using the quasi-static approximation. We model the tip as a prolate spheroid with conductivity and dielectric constant related to the plasma parameters. The main result of this model is the field enhancement near the tip by an amount related to the tip radius and the distance from the tip. To obtain a clear, yet representing, one dimensional model of the acceleration process, we analyze the interaction of the laser with the plasma distributed along one ray in parallel to the laser wave-vector. The density profile of the plasma along a ray and the enhancement factor of the laser amplitude due to the tip are described in Fig. 6. We now solve a set of one-dimensional fluid equations for the electrons and ions in plasma of the given distribution function assuming that the main pulse propagates from the left edge to the right and is subject to the tip enhancement. The effect of the ponderomotive potential in this case is enhanced by two factors. First is the local field enhancement which is translated to direct enhancement of the amplitude. Next is the increment of the gradient of the ponderomotive potential due to the local character of the field enhancement. The plasma electrons are therefore subjected to a greatly increased force and accordingly the density is modified to a greater extent than is expected of the laser intensity by itself. Fig. 6 demonstrates this enhancement. Black line shows the distribution of the electrons after the passage of the laser pulse including the tip enhancement. The exact position and magnitude of the electron cloud is a function of the maximal enhancement and gradient of the tip. We note that the level to which the electrons are compressed depends also on the temperature they gain in the process. Up to this stage the ions are practically not affected by the laser pulse at all. However, they start to respond to the electrostatic potential of the electrons cloud. Following the conventional model [13], we estimate the temperature of the electrons in the cloud, the scale length that determines the intensity of the accelerating field and the accelerating distance. To estimate the temperature of the electrons we use the following expression:

$$kT_{\text{hot}} \sim m_e c^2 \left[ \sqrt{1 + \frac{a_{\text{tip}}^2 I \lambda^2}{1.37 \times 10^{18}}} - 1 \right]$$

Here the conventional scaling of the laser intensity is multiplied by the field enhancement of the tip,  $a_{\text{tip}}$  (squared for intensity). Taking this factor to be 10 (which means a modest field enhancement of  $\sim 3$ ) we find that the temperature of the hot electrons in the cloud is of the order of 200-300 keV. Next we estimate the scale length of the local plasma using the calculations of the cold fluid model. Based on the fluid model we find that the electrons cloud is ramped up by a steep gradient which is estimated to be 0.1-0.05  $\lambda$  (see Fig. 6). Furthermore, we estimate that the length over which the protons can be accelerated is  $\lambda$ . Combining the above we find that the protons can be accelerated to about 10-20  $kT_{\text{hot}}$  which for laser intensity at the range of  $4.5 \times 10^{17}$  W/cm<sup>2</sup> is 2-6 MeV. Several remarks are in order. First, we would like to stress that the most energetic protons are accelerated in a direction that is defined by the orientation between the tip and the wave vector of the laser. This is supported by our experimental results where we find bunches of accelerated protons and not a uniform distribution. Furthermore, as this acceleration scheme is ballistic in nature we do not expect a large amount of protons to reach this energy unless specially designed targets are used.

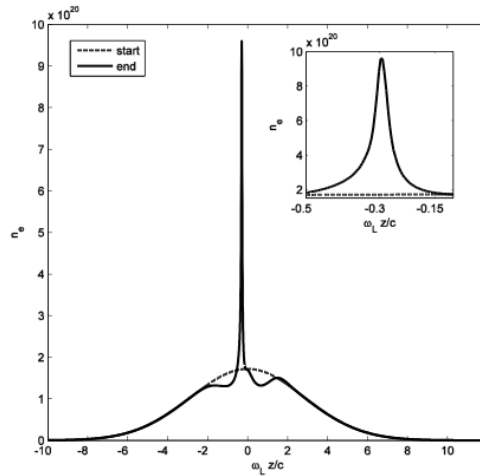


**FIGURE 6.** Electron density normalized to the laser frequency before and after the main laser pulse has passed the H<sub>2</sub>O nanowire. Inset: Zoom on the region of peak electron density

We have experimentally demonstrated generation of 5.5-7.5 MeV protons from snow nanowire targets by modest,  $4.5 \times 10^{17}$  W/cm<sup>2</sup> laser intensities, and up to 12 MeV with  $1.5 \times 10^{18}$  W/cm<sup>2</sup>. The protons are accelerated by the enhanced interaction of the laser field and the plasma near the tip of the nanowire.

## REFERENCES

1. Hegelich, B. M. et al. Laser acceleration of quasi-monoenergetic MeV ion beams. *Nature* **439**, 26 (2006).
2. Schwoerer, H. et al. Laser-plasma acceleration of quasi-monoenergetic protons from microstructured targets. *Nature* **439**, 445 (2006).
3. Fuchs, J, et al. Laser acceleration of low emittance, high energy ions and applications. *C. R. Physique* **10**, 176 (2009).
4. Hatchett, S. et al. Electron, photon, and ion beams from the relativistic interaction of Petawatt laser pulses with solid targets. *Phys. Plasmas* **7**, 2076 (2000).
5. Wilks, S. et al. Energetic proton generation in ultra-intense laser-solid interactions. *Phys. Plasmas* **8**, 542 (2001).
6. Gaillard, S. A. et al. 65+ MeV protons from short-pulse-laser micro-cone-target interactions. In Proc. APS 51<sup>st</sup> Annual meeting of the APS Division of Plasma Physics, Abstract G06.003 (2009).
7. Bagchi, S. et al. Fast ion beams from intense, femtosecond laser irradiated nanostructured surfaces. *Appl. Phys. B* **88**, 167-173 (2007)
8. Ramakrishna, B. et al. Laser-driven quasimonoenergetic proton burst from water spray target. *Phys. Plasmas* **17**, 083113 (2010)
9. Palchan, T. et. al. Efficient coupling of high intensity short laser pulses into snow clusters. *App. Phys. Lett.* **90**, 041501 (2007).
10. Palchan, T. et. al. Generation of fast ions by an efficient coupling of high power laser into snow nanotubes. *App. Phys. Lett.* **91**, 251501 (2007).
11. Borghesi, M. et al. Fast ion generation by high-intensity laser irradiation of solid target and applications. *Fusion Sci. Technol.* **49**, 412 (2006)
12. A. Zigler, T. Palchan, N. Bruner, E. Schleifer et al., *Phys. Rev. Lett.* **106**, 134801 (2011)
13. Wilks, S. C. and Kruer, W.L. *IEEE J Quantum Elect.* **33**, 1954 (1997).